Eur Radiol (2017) 27:4819–4827
DOI 10.1007/s00330-017-4898-5

BREAST

Additional value of diffusion-weighted imaging to evaluate multifocal and multicentric breast cancer detected using pre-operative breast MRI

Sung Eun Song[1] · Eun Kyung Park[1] · Kyu Ran Cho[1] · Bo Kyoung Seo[2] · Ok Hee Woo[3] · Seung Pil Jung[4] · Sung Bum Cho[1]

Received: 2 March 2017 / Revised: 2 May 2017 / Accepted: 12 May 2017 / Published online: 7 June 2017

Abstract

Objectives To investigate whether diffusion-weighted imaging (DWI) aids pre-operative dynamic contrast-enhanced magnetic resonance imaging (DCE-MRI) to evaluate additional lesions in breast cancer patients.

Methods DCE-MRI and DWI were performed on 131 lesions, with available histopathological results. The apparent diffusion coefficient (ADC) of each lesion was measured, and the cut-off value for differentiation between malignant and benign lesions was calculated. A protocol combining the ADC cut-off value with DCE-MRI was validated in a cohort of 107 lesions in 77 patients.

Results When an ADC cut-off value of 1.11×10^{-3} mm^2/s from the development cohort was applied to the additional lesions in the validation cohort, the specificity increased from 18.9% to 67.6% ($P < 0.001$), and the diagnostic accuracy increased from 61.7% to 82.2% ($P = 0.05$), without significant loss of sensitivity (98.6% vs. 90.0%, $P = 0.07$). The negative predictive values of lesions in the same quadrant had decreased, as had those of lesions ≥1 cm in diameter. The ADC cut-off value in the validation cohort was 1.05×10^{-3} mm^2/s.

Conclusions Additional implementation of DWI for breast lesions in pre-operative MRI can help to obviate unnecessary biopsies by increasing specificity. However, to avoid missing cancers, clinicians should closely monitor lesions located in the same quadrant or lesions ≥1 cm.

Key Points

- *DWI can be used to further differentiate lesions during pre-operative cancer staging.*
- *ADC cut-off values were similar in the development and validation cohorts.*
- *DWI improves both PPV and NPV in cases of multicentric lesions.*
- *DWI improves both PPV and NPV in lesions <1 in diameter.*
- *NPVs are decreased in multifocal lesions and lesions ≥1 cm in diameter.*

Keywords Breast neoplasm · Diffusion-weighted imaging · Breast magnetic resonance imaging · Apparent diffusion coefficient · Staging

Sung Eun Song and Eun Kyung Park contributed equally to this work.

✉ Kyu Ran Cho
krcho@korea.ac.kr

[1] Department of Radiology, Korea University Anam Hospital, Korea University College of Medicine, 73, Inchon-ro, Seongbuk-gu, Seoul 02841, Korea

[2] Department of Radiology, Korea University Ansan Hospital, Korea University College of Medicine, Ansan, Korea

[3] Department of Radiology, Korea University Guro Hospital, Korea University College of Medicine, Seoul, Korea

[4] Department of Surgery, Korea University Anam Hospital, Korea University College of Medicine, Seoul, Korea

Introduction

Dynamic contrast-enhanced magnetic resonance imaging (DCE-MRI) has become an important imaging tool for breast cancer staging [1–3] because the technique has high sensitivity, which allows detection of additional lesions that are undetectable by mammography or ultrasound (US) in 6%–34% of cases [4]. However, the reported specificity of DCE-MRI ranges from 37% to 97%, so additional lesions in breast cancer patients should always be confirmed histopathologically to rule out multifocal or multicentric cancers [5, 6]. Indeed, histologically confirmed multifocal or multicentric breast cancers

occur in 21%–63% of affected breasts [7, 8]. Although the American Joint Committee on Cancer (AJCC) staging system does not consider whether the disease is multifocal or multicentric [9], such findings are known to be associated with worse breast cancer-specific and relapse-free survival [10]. Furthermore, multifocality and multicentricity in breast cancer affect the decisions surrounding surgical management, such as whether to perform mastectomy or breast-conserving surgery [10].

Multiparametric MRI, which derives diagnostic information from both morphologic and functional MRI parameters, has increased the accuracy of breast cancer diagnosis [11, 12]. Among the functional MRI parameters used, diffusion-weighted imaging (DWI) has become important in clinical practice; DWI provides apparent diffusion coefficient (ADC) values, which differ significantly between benign and malignant lesions [13, 14]. Moreover, combining DWI with conventional DCE-MRI improves diagnostic accuracy and reduces the number of false diagnoses [11, 12, 15]. However, no previous investigations have validated whether DWI could also be used to evaluate additional suspicious lesions detected using DCE-MRI in patients with breast cancer, thus revealing multifocality or multicentricity. Therefore, the purpose of this study was to investigate whether DWI adds value to pre-operative DCE-MRI in the evaluation of additional lesions in patients with breast cancer.

Materials and methods

This prospective study was approved by the institutional review board (IRB number: ED 14341). Since 2013, our hospital has offered DWI, in addition to DCE-MRI, to women scheduled for breast cancer surgery.

Study populations and breast lesions

Development cohort

Between July 2014 and February 2015, 96 consecutive women with newly diagnosed breast cancer underwent pre-operative DCE-MRI and DWI. Among them, we excluded women who (1) were not to undergo surgery in our institution (n = 13), (2) had motion artefacts (n = 5), and (3) had undergone excisional biopsy prior to MRI (n = 2). Ultimately, the development set consisted of 76 women (mean age: 54 years, range: 32–83 years) with 131 breast lesions (mean diameter: 1.7 cm, range: 0.5–7.0 cm), all of which had final pathology results available. Of the 131 breast lesions, 106 (80.9%) were malignant and 25 (19.1%) were benign. The apparent diffusion coefficient (ADC) of each lesion was measured, and a cut-off value for differentiation between malignant and benign lesions was calculated using receiver-operating characteristic (ROC) curve analysis. The ADC value from the development set was applied prospectively to a validation set.

Validation cohort

After an interval of 1 month, we prospectively enrolled patients with breast cancer who were to undergo pre-operative DCE-MRI and DWI between March and October 2015. In this way, we investigated the diagnostic performance of the combined protocol by combining the ADC cut-off value with DCE-MRI. Among 102 consecutive women with breast cancer who underwent pre-operative DCE-MRI, we excluded 25 who fulfilled the above-mentioned criteria. The remaining 77 women had 117 additional lesions—detected using pre-operative breast MRI. Of these 117 additional lesions, 10 (8.5%) were excluded from this study because they were not precisely found or biopsied. Ultimately, 107 additional lesions in 77 women (mean age: 48.8 years; range: 32–76 years) were included, and all lesions were verified by performing pathological analysis.

Magnetic resonance imaging

A 3.0-T system (Achieva 3.0 T TX; Philips Healthcare) with a dedicated, phased-array breast coil was used for DCE-MRI; patients were placed in the prone position. DWI was acquired in the transverse plane. A spin-echo, single-shot, echo-planar-imaging sequence, with diffusion-sensitising gradients, was applied along the orthogonal directions. The images thus obtained were used to synthesise isotopic transverse images [repetition time (ms)/echo time (ms): 12,500/58; flip angle 90°; SPAIR fat suppression; in-plane resolution 1.15 mm × 1.15 mm; 50 slices; b-values: 0, 600 and 1000 s/mm^2; image matrix: 128 × 128; field of view: 320 × 320 mm; section thickness: 3 mm; section gap: 0 mm; SENSE factor = 2.3, two averages; three signals acquired; acquisition time: 80 s]. After DWI, T2-weighted, fast spin-echo, transverse images were obtained [repetition time (ms)/echo time (ms): 5727/70; flip angle: 90°; image matrix: 620 × 309; field of view: 581 × 342 mm; section thickness: 3 mm; section gap: 0 mm]. For DCE-MRI, one pre-contrast and six post-contrast dynamic series were performed using a three-dimensional, T1-weighted, fast spoiled gradient-echo sequence (6/3; flip angle: 10°: 100 slices: image matrix: 436 × 436; field of view: 330 × 340 mm; section thickness: 1.5 mm; no gap) immediately after and at 60, 120, 180, 240, and 300 s after the contrast injection.

Magnetic resonance image analysis

Two breast radiologists (S.E.S., E.K.P.) with 6 and 3 years of experience in breast radiology, respectively, prospectively assessed the characteristics of each lesion, reaching a

consensus in each case. Their analysis was based on morphological and kinetic criteria and it used the breast imaging reporting and data system (BI-RADS) MRI atlas of the American College of Radiology [16]. In accordance with the BI-RADS atlas, the following descriptors were used to analyse the masses: shape, margin, and internal enhancement; similarly, the following descriptors were used to analyse non-mass enhancement (NME): distribution and internal enhancement pattern. The enhancement kinetic curve was evaluated using a computer-aided detection (CAD) system (CADstream software, version 5.2.8.591; Merge Healthcare, Chicago, IL, USA). The type of curve was defined in terms of the single most suspicious enhancement: type I (low persistent), type II (medium, fast persistent, or plateau), and type III (medium or fast washout). Based on previous positive predictive value (PPV) results suggesting malignancy on the basis of MRI findings [16–18], the final assessment category of each lesion was defined as follows: 3, probably benign enhancement; 4, suspicious; 5, highly suggestive of malignancy.

Diffusion-weighted imaging and ADC analysis

The ADC maps were constructed using a commercially available CAD system using *b*-values of 0 and 1000 s/mm^2. When each additional breast lesion with a BI-RADS category of 3, 4, or 5 was detected on the colour map using the CAD system, the ADC map was placed beside the colour map. One breast radiologist (E.K.P.), with 3 years' experience in breast radiology, manually outlined the regions of interest (ROIs) and measured the ADC value, using the CAD system to cover the entire tumour in its three largest cross-sections. The measurements were performed three times, and the average value was defined as the ADC of each lesion.

Combined analysis using DCE-MRI and DWI

To carry out the combined analysis of DCE-MRI and DWI, we used an algorithm adapted from the BI-RADS atlas [11, 12, 16], in which the ADC cut-off values acquired from the development set were applied to the validation set to estimate the likelihood of malignancy in any additional lesions with a given BI-RADS assessment category. For example, in the case of BI-RADS assessment category 3, a lower ADC cut-off value was required in the development set to upgrade a lesion to malignant status. In the case of BI-RADS assessment categories 4 or 5, a higher ADC cut-off value was required in the development set to downgrade a lesion to "probably benign" status.

Histopathological Analysis

To carry out histopathological diagnosis, image-guided core biopsies, or image-guided needle-localisation and excisional biopsies, were performed on all lesions. Pathological specimens were obtained within 1–2 weeks of the pre-operative MRI scans. In the case of breast-conserving surgery, specimens were prepared as serial 5-mm slices; mastectomy specimens were prepared as 5–10-mm slices [19]. To determine whether pathological features corresponded with the findings of breast imaging, pathologists, breast surgeons, and radiologists reviewed all specimens together. The pathologists were then asked to assess the additional suspicious lesions separately to evaluate multifocality and multicentricity.

Data analysis

In the development cohort, a receiver-operating characteristic (ROC) curve was constructed to determine the ADC cut-off value, which was used to differentiate benign from malignant lesions. In the validation cohort, the combined protocol, which considered both the ADC cut-off value and DCE-MRI, was evaluated. Breast lesions with an ADC value above the cut-off were reclassified as negative, and those with an ADC value below the cut-off were reclassified as positive. Sensitivity, specificity, PPV, negative predictive value (NPV), and accuracy of both DCE-MRI and the combined protocol were calculated; sensitivity, specificity, and accuracy were compared using McNemar's test. In the validation cohort, ROC curve analysis was also performed. All statistical analyses were performed using statistical software (SPSS, version 20.0; SPSS Chicago, IL, USA), and a P-value < 0.05 denoted significance.

Results

DWI and ROC analysis in the development cohort

Of the 131 breast lesions in the development cohort, 106 (80.9%) were malignant and 25 (19.1%) were benign. Among the 106 malignant lesions, 92 (86.8%) were invasive carcinomas and 14 (13.2%) were ductal carcinomas *in situ* (DCISs). The mean ADC of the malignant lesions was $0.93 \pm 0.16 \times 10^{-3}$ mm^2/s and that of benign lesions was $1.20 \pm 0.26 \times 10^{-3}$ mm^2/s (Fig. 1). The ADC values were significantly lower in the malignant lesions than in the benign lesions ($P < 0.01$). The best ADC cut-off to differentiate benign from malignant lesions, as determined using ROC-curve analysis, was 1.11×10^{-3} mm^2/s, which yielded a sensitivity of 87.0% and a specificity of 67.2%. The area under the ROC curve for differentiating benign from malignant lesions was 0.810 (95% confidence interval: 0.766–0.898).

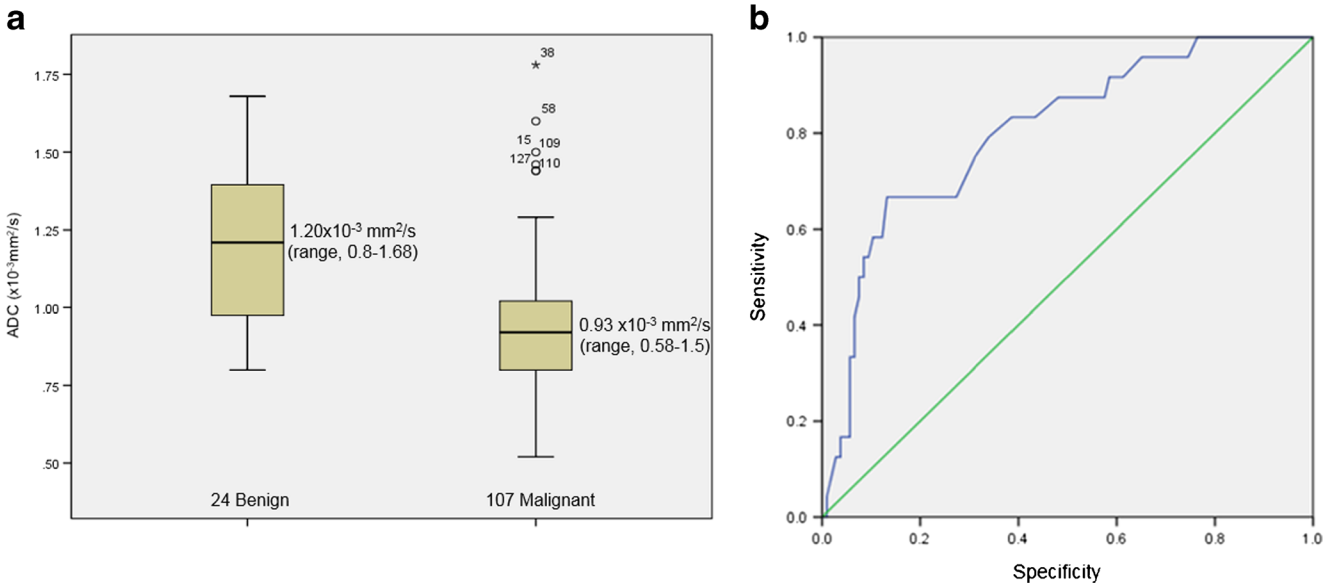

Fig. 1 ADC values from the development cohort. (**a**) Graph showing the mean ADC values of benign versus malignant breast lesions. The mean ADC value of the malignant lesions ($0.93 \pm 0.16 \times 10^{-3}$ mm^2/s) was significantly lower than those of benign lesions ($1.20 \pm 0.26 \times 10^{-3}$ mm^2/s, $P < 0.01$). (**b**) The best ADC cut-off value to differentiate benign from malignant lesions, as determined using ROC curve analysis, was 1.11×10^{-3} mm^2/s. The area under the ROC curve to differentiate benign from malignant lesions was 0.810

DCE-MRI in the validation cohort

Among the 107 additional lesions in the validation cohort, histopathological analysis revealed 70 malignant lesions (mean diameter: 1.0 cm, range: 0.5–4.2 cm) and 37 benign lesions (mean diameter: 0.9 cm, range: 0.5–2.3 cm). The malignant lesions comprised 61 invasive cancers (50 invasive ductal carcinomas, 6 invasive micropapillary carcinomas, two invasive medullary carcinomas, two invasive cribriform carcinomas, and one invasive mucinous carcinoma) and 9 DCISs. The benign lesions comprised 26 cases of fibrocystic change, three fibroadenomas, three cases of sclerosing adenosis, three cases of usual ductal hyperplasia, and two benign intraductal papillomas.

There were 95 masses (mean diameter: 0.9 cm, range: 0.5–2.4 cm) and 12 NME lesions (mean: 1.7 cm, range: 0.7–4.2 cm). Eight lesions (7.5%) were assigned the BI-RADS final assessment category 3; 73 lesions (68.2%) were defined as category 4, and 26 lesions (24.3%) were placed in category 5 (Table 1). All benign lesions that were not excised but biopsied showed stability after a median 15-month follow-up period. DCE-MRI showed 98.6% sensitivity, 18.9% specificity, 69.6% PPV, 87.5% NPV, and 61.7% diagnostic accuracy (Table 2).

Combined analysis using DCE-MRI and DWI in the validation set

When DWI was applied to DCE-MRI using the best ADC cut-off value (1.11×10^{-3} mm^2/s), as derived from the development cohort, 21 false-positive DCE-MRI findings with BI-RADS category 4 became true-negative findings (Fig. 2; Table 3) and 3 true-negative DCE-MRI findings with BI-RADS category 3 became false-positive findings. With application of DWI, 3 of 26 lesions with BI-RADS category 5 and 4 of 43 lesions with BI-RADS category 4 in DCE-MRI were downgraded to probably benign status and became false-negative findings (Table 4). Specifically, the combined MRI protocol conferred 90.0% sensitivity, 82.2% specificity, 92.0% PPV, 78.1% NPV, and 82.2% diagnostic accuracy. The addition of DWI to DCE-MRI conferred a 63.3% increase in the specificity ($P < 0.001$) and a 20.5% increase in the diagnostic accuracy ($P = 0.05$), without significantly decreasing the sensitivity ($P = 0.07$).

Malignancy rate and performance in multifocal and multicentric breast cancer

Of the 107 additional lesions, 60 (56.0%) were located in the same quadrant of the affected breast; 47 (44.0%) were located in a different quadrant. Of the 60 lesions in the same quadrant, 52 (86.6%) were malignant (47 invasive cancers, 5 DCISs). Of the 47 lesions in a different quadrant, 18 (48.6%) were malignant (14 invasive cancers, 4 DCISs; Fig. 3). The malignancy rate of the multifocal lesions was 86.6%, while that of the multicentric additional lesions was 48.6%. In the case of lesions in the same quadrant, DCE-MRI showed 100% sensitivity, 21.4% specificity, 82.5% PPV, 100% NPV, and 83.3% overall accuracy. The combined protocol conferred 90.4%

Table 1 Lesion characteristics of 107 additional lesions in the validation cohort

	Benign (n = 37)	Malignancy (n = 70)
MRI features		
Mass	32	63
Shape		
Oval	13	15
Round	18	42
Irregular	1	6
Margin		
Circumscribed	9	3
Irregular	23	45
Spiculated	0	15
Internal enhancement patterns		
Homogeneous	17	8
Heterogeneous	13	50
Rim enhancement	2	5
Non-mass enhancement	5	7
Distribution		
Focal	4	
Linear	1	3
Segmental	0	3
Regional	0	1
Internal enhancement patterns		
Heterogeneous	4	3
Clumped	0	1
Clustered ring	1	3
Kinetic feature using CAD[a]		
Type I (low persistent)	21	8
Type II (medium, fast persistent or plateau)	4	29
Type III (medium or fast washout)	12	33
BI-RADS category		
Category 3	7	1
Category 4	30	43
Category 5	0	26

[a] CAD, Computer-aided detection

sensitivity, 78.5% specificity, 94.0% PPV, 68.7% NPV, and 87.8% overall accuracy; the specificity was significantly higher in the combined protocol (P = 0.008). However, NPV decreased from 100% to 68.7%. Five of 16 (31.3%) multifocal lesions were missed by the use of the combined protocol (Table 4). In the case of lesions in a different quadrant, DCE-MRI showed 94.4% sensitivity, 17.3% specificity, 47.2% PPV, 80% NPV, and 51.2% overall accuracy. The combined protocol conferred 88.8% sensitivity, 60.8% specificity, 64.0% PPV, 87.5% NPV, and 73.1% overall accuracy; the specificity was significantly higher in the combined protocol (P = 0.021).

Table 2 Diagnostic performance of combined DCE-MRI and MRI protocol in 107 additional lesions

Results	DCE-MRI	Combined protocol	P-value
True positive*	69	63	-
True negative*	7	25	-
False positive*	30	12	-
False negative*	1	7	-
PPV[a] (%)	69.6%	84.0%	-
NPV[b] (%)	87.5%	78.1%	-
Sensitivity (%)	98.6%	90.0%	0.07
Specificity (%)	18.9%	67.6%	<0.001
Overall accuracy (%)	61.7%	82.2%	0.05

* Data are number of lesions.

[a] PPV, Positive predictive value; [b] NPV, negative predictive value

Comparison of performance according to lesion size

Of the 107 lesions, 41 (38.3%) were large (≥1 cm in diameter) and 66 (61.7%) were small (<1 cm in diameter). In the case of large lesions, DCE-MRI showed 100% sensitivity, 16.6% specificity, 74.3% PPV, 100% NPV, and 75.6% overall accuracy. The combined protocol conferred 82.7% sensitivity, 91.6% specificity, 96.0% PPV, 68.7% NPV, and 85.4% overall accuracy; the specificity was significantly higher in the combined protocol (P = 0.004). However, NPV decreased from 100% to 68.7%. Five of 16 (31.3%) large lesions were missed precisely because DWI was applied (Table 4). In the case of small lesions, DCE-MRI showed 97.6% sensitivity, 20.0% specificity, 66.6% PPV, 83.3% NPV, and 68.1% overall accuracy. The combined protocol showed 95.1% sensitivity, 56.0% specificity, 78.0% PPV, 87.5% NPV, and 80.3% overall accuracy; the specificity was significantly higher in the combined protocol (P = 0.035).

Discussion

Not only has breast MRI improved cancer detection, but it has also yielded substantial numbers of unpredictable lesions with low PPV [5, 6, 20]. Several researchers have suggested combining DWI with DCE-MRI to help distinguish malignant lesions from benign lesions and to reduce the number of false positives [11–15]. Furthermore, some recent studies have reported improved specificity in the characterisation of breast tumours—from 13.5% to 89% [21] and from 22% to 78% [11]—when the ADC cut-off was applied to the DCE-MRI classification. Spick et al. [15] also reported that applying DWI to suspicious lesions visible on DCE-MRI may prevent unnecessary biopsies in up to 34.5% of cases. However, to our knowledge, the present study was the first to evaluate the

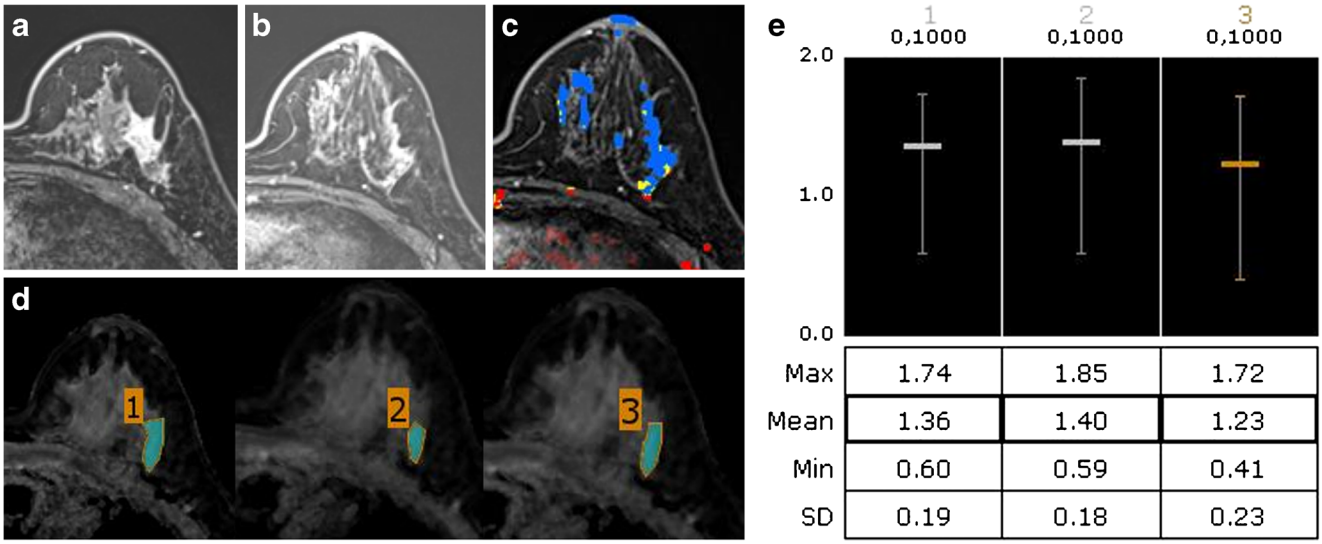

Fig. 2 A 47-year-old female with left-breast cancer. (**a**) Contrast-enhanced, fat-suppressed, T1-weighted, axial MR image showing an irregular-shaped and marginated mass with heterogeneous enhancement in the left upper outer breast. (**b**) A regional non-mass enhancement 2.2 cm in diameter in the lower portion of the same quadrant as known cancer. (**c**) Colour map created using CAD showing the same non-mass enhancement with a predominantly blue overlay, indicating that the kinetic pattern was persistent. (**d**) To measure the ADC value, the regions of interest are manually outlined, ensuring that the entire tumour is covered in the three largest cross-sections. (**e**) The average ADC is 1.33 × 10^{-3} mm^2/s, and the lesion appears as fibrocystic change after excision

usefulness of DWI in pre-operative breast cancer staging. Overall diagnostic accuracy and specificity were significantly improved in our combined protocol, without significant loss of sensitivity, when additional lesions that showed an ADC

Table 3 Reduction of false-positive cases by combining the ADC value of diffusion-weighted imaging and DCE-MRI

No.	Age	Size (mm)	MRI features (mass/NME[a])	Quadrant (same/different)	BI-RADS category in DCE-MRI	ADC[b] value (×10^{-3} mm^2/s)	BI-RADS Category in combined protocol	Histology
1	45	7	Mass	Different	BI-RADS 4	1.22	BI-RADS 3	Usual ductal hyperplasia
2	35	8	Mass	Different	BI-RADS 4	1.24	BI-RADS 3	Fibrocystic change
3	35	6	Mass	Different	BI-RADS 4	1.25	BI-RADS 3	Fibrocystic change
4	35	8	Mass	Different	BI-RADS 4	1.41	BI-RADS 3	Usual ductal hyperplasia
5	47	23	NME	Same	BI-RADS 4	1.33	BI-RADS 3	Fibrocystic change
6	44	17	Mass	Different	BI-RADS 4	1.30	BI-RADS 3	Fibrocystic change
7	56	7	NME	Same	BI-RADS 4	1.60	BI-RADS 3	Fibrocystic change
8	44	7	Mass	Same	BI-RADS 4	1.20	BI-RADS 3	Fibrocystic change
9	46	13	NME	Different	BI-RADS 4	1.26	BI-RADS 3	Fibrocystic change
10	51	13	NME	Same	BI-RADS 4	1.18	BI-RADS 3	Usual ductal hyperplasia
11	42	7	Mass	Same	BI-RADS 4	1.16	BI-RADS 3	Fibrocystic change
12	43	10	Mass	Different	BI-RADS 4	1.12	BI-RADS 3	Sclerosing adenosis
13	43	6	Mass	Different	BI-RADS 4	1.21	BI-RADS 3	Fibroadenoma
14	39	8	Mass	Different	BI-RADS 4	1.18	BI-RADS 3	Fibrocystic change
15	35	7	Mass	Different	BI-RADS 4	1.71	BI-RADS 3	Fibroadenoma
16	48	7	Mass	Same	BI-RADS 4	1.18	BI-RADS 3	Fibrocystic change
17	48	10	Mass	Same	BI-RADS 4	1.13	BI-RADS 3	Fibrocystic change
18	48	11	Mass	Different	BI-RADS 4	1.32	BI-RADS 3	Fibrocystic change
19	46	6	Mass	Same	BI-RADS 4	1.26	BI-RADS 3	Fibrocystic change
20	47	10	Mass	Different	BI-RADS 4	1.22	BI-RADS 3	Fibrocystic change
21	45	10	Mass	Different	BI-RADS 4	1.17	BI-RADS 3	Fibrocystic change

[a] NME, Non-mass enhancement; [b] ADC, apparent diffusion coefficient

Table 4 False-negative cases by combining the ADC value of diffusion-weighted imaging and DCE-MRI

No.	Age	Size (mm)	MRI features (mass/NME[a])	Quadrant (same/different)	BI-RADS category in DCE-MRI	ADC[b] value ($\times 10^{-3}$ mm^2/s)	BI-RADS category in combined protocol	Histology
1	42	42	NME	Different	BI-RADS 5	1.46	BI-RADS 3	Ductal carcinoma in situ
2	42	18	NME	Different	BI-RADS 5	1.44	BI-RADS 3	Ductal carcinoma in situ
3	43	16	Mass	Same	BI-RADS 5	1.35	BI-RADS 3	Invasive ductal carcinoma
4	43	12	NME	Same	BI-RADS 4	1.42	BI-RADS 3	Ductal carcinoma in situ
5	45	23	Mass	Same	BI-RADS 4	1.21	BI-RADS 3	Ductal carcinoma in situ
6	76	8	Mass	Same	BI-RADS 4	1.33	BI-RADS 3	Invasive ductal carcinoma
7	40	7	Mass	Same	BI-RADS 4	1.37	BI-RADS 3	Ductal carcinoma in situ

[a] NME, Non-mass enhancement; [b] ADC, apparent diffusion coefficient

value of $<1.11\times10^{-3}$ mm^2/s were considered malignant. Recommended ADC cut-off values for differentiation between benign and malignant breast lesions varied from 0.90 to 1.76 × 10^{-3} mm^2/s [22]. Another meta-analysis of 12 articles using a b value of 0, 1000 s/mm^2 on 1.5 T recommended an ADC cut-off value of 1.23 × 10^{-3} mm^2/s [23]. Cakir et al. [24] using a b value of 0, 1000 s/mm^2 on 3.0-T suggested an ADC value of 1.12 × 10^{-3} mm^2/s with diagnostic accuracy of 82%, which was similar to our ADC value of 1.11 × 10^{-3} mm^2/s and diagnostic accuracy of 82.2%. The main strength of our study was that the results were not derived from a single cohort; instead, they were validated using another cohort. Moreover, the cut-off values in both cohorts were very similar (1.11×10^{-3} mm^2/s from the development cohort and 1.05×10^{-3} mm^2/s from the validation cohort). In the present study, DCE-MRI led to 30 false-positive findings; the combined protocol helped to reduce this number to only 12 false-positive findings. Therefore, if DWI is combined with pre-operative MRI when breast cancer patients show additional lesions, unnecessary biopsies or extensive surgery could be avoided.

Patients with multifocal or multicentric cancers should be treated with a mastectomy rather than with wide excisions because there is a higher risk of local recurrence and because a worse cosmetic outcome is expected [25]. In one study, treatment was converted from breast conserving therapy to mastectomy in 8.1% of cases because of multifocality or multicentricity [8]. For this reason, histopathological confirmation of additional lesions should be performed in patients with breast cancer. In a meta-analysis by Houssami et al. [8], DCE-MRI of additional lesions in patients with breast cancer

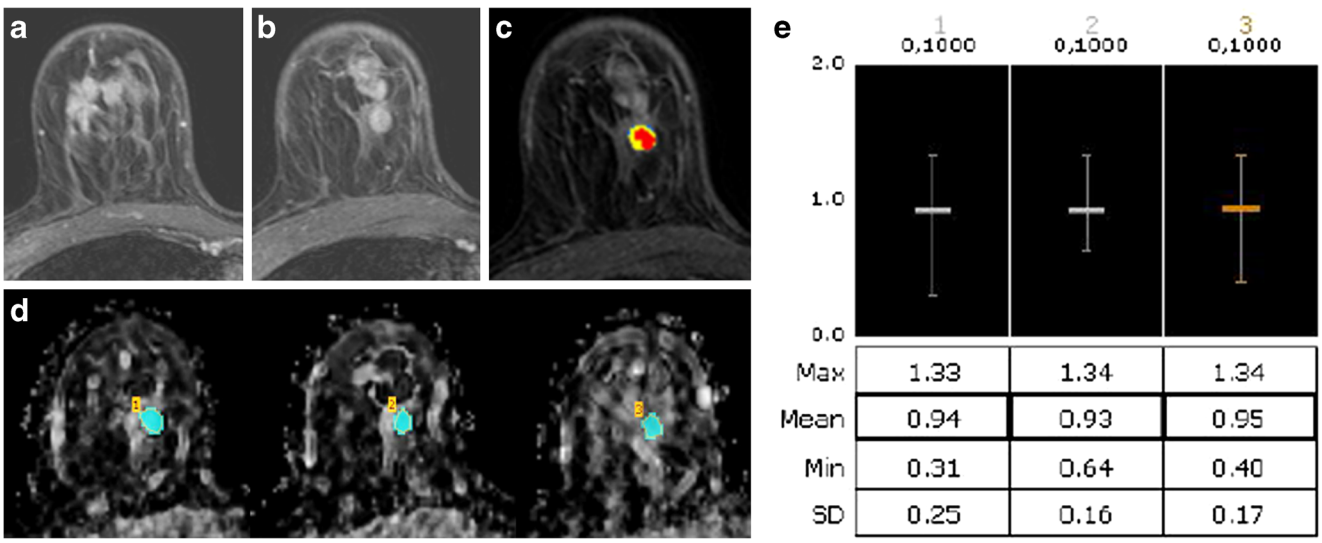

Fig. 3 A 46-year-old female with right-breast cancer (**a**) Contrast-enhanced, fat-suppressed, T1-weighted axial MR image showing an irregular-shaped, spiculated-marginated mass with heterogeneous enhancement in the right upper outer breast. (**b**) Oval, circumscribed, heterogeneously enhancing mass, 0.9 cm in diameter, is seen in the right upper inner breast. (**c**) Colour map created using CAD showing the mass with a predominantly red overlay and indicating the washout kinetic pattern. (**d**) To measure the ADC value, the regions of interest are manually outlined, ensuring that the entire tumour is covered in the three largest cross-sections. (**e**) The average ADC is 0.94 × 10^{-3} mm^2/s, and the lesion is revealed as an invasive ductal carcinoma after excision

had a PPV of 66%. In the present study, the PPV of DCE-MRI alone was higher (82.5%) in the case of multifocal lesions, but lower (47.2%) in the case of multicentric lesions. In the combined protocol, both the PPV (47.2% to 64.0%) and NPV (80.0% to 87.5%) had increased in the case of multicentric lesions; however, in the case of multifocal cancers, the NPV had decreased from 100% to 68.7%, while the PPV had increased from 82.5% to 94.0%. Five of 16 (31.3%) multifocal lesions were missed by the use of the combined protocol. Considering the malignancy rates of multifocal and multicentric lesions in the present study were 86.6% and 48.6%, respectively, DWI could be used alongside pre-operative MRI to inform decisions about whether multicentric lesions should be excised or biopsied; however, the same does not apply in the case of multifocal lesions.

We further compared the diagnostic performance of the protocols according to lesion size. The combined protocol consistently increased the PPV, regardless of lesion size, although the PPV of small lesions was lower than that of large lesions (78.0% vs. 96.0%). Another important finding in the present study was that the NPV of larger lesions (≥1 cm in diameter) had decreased from 100% when using DCE-MRI to 68.7% when using the combined protocol, while the NPV of small lesions (<1 cm in diameter) had increased from 83.3% to 87.5%. In the present study, 5 of 16 (31.3%) large lesions were missed precisely because DWI was applied. Therefore, when applying the ADC value to DCE-MRI, physicians should pay close attention to lesions ≥1 cm in diameter to avoid missing cancers on pre-operative breast MRI.

There were several limitations in this study. First, lesions that were probably benign, but that lacked pathological diagnosis, were excluded, as were several additional lesions that were detected using MRI, but were not found or biopsied. This may have led to selection bias. Second, the number of benign lesions within the total sample size was small. Third, the ADC values of benign lesions in our study seem to be low compared with those in the published literature. Methods for selecting a suitable ROI within a lesion for measuring of the ADC values are varied and rather subjective. So, we used a CAD system. The reason for low ADC values in our study was assumed to be that we measured the ADC values by outlining the ROIs to cover the entire tumour with a colour map above the set enhancement threshold of a CAD. It enabled measuring the lesions without including surrounding breast tissues, resulting in low ADC values. Fourth, the DWI acquisition resolution was 1.15 m ×1.15 mm, and the smallest lesions in our study were 5-6 mm in diameter; thus we measured the ADC values on the basis of 4-5 acquisition pixels, which was a risky undertaking. Fifth, we did not assess inter- or intra-observer agreement with regard to ADC measurement.

In conclusion, MRI staging leads to unnecessarily extensive breast surgery in a considerable proportion of patients because it allows the detection of additional lesions. Therefore, it is necessary to reduce the number of false-positive additional lesions detected using pre-operative MRI. Our current findings indicate that, with the implementation of DWI to additional lesions in patients with breast cancer, unnecessary biopsies or extensive surgery could be avoided. However, when we applied the ADC value to DCE-MRI, we found that, to avoid missing cancers, physicians should pay close attention to additional lesions located in the same quadrant as the confirmed cancer, as well as to those >1 cm in diameter, because such lesions have reduced NPVs and because the malignancy rate of lesions in the same quadrant as the original cancer is 86.6%.

Compliance with ethical standards

Guarantor The scientific guarantor of this publication is Kyu Ran Cho.

Conflict of interest The authors of this manuscript declare no relationships with any companies, whose products or services may be related to the subject matter of the article.

Funding The authors state that this work has not received any funding.

Statistics and biometry No complex statistical methods were necessary for this paper.

Informed consent Written informed consent was obtained from all subjects (patients) in this study.

Ethical approval Institutional Review Board approval was obtained.

Methodology
- prospective
- observational
- performed at one institution

References

1. Orel SG, Schnall MD (2001) MR imaging of the breast for the detection, diagnosis, and staging of breast cancer. Radiology 220: 13–30
2. Orel SG, Schnall MD, LiVolsi VA, Troupin RH (1994) Suspicious breast lesions: MR imaging with radiologic-pathologic correlation. Radiology 190:485–493
3. Harms SE, Flamig DP, Hesley KL et al (1993) MR imaging of the breast with rotating delivery of excitation off resonance: clinical experience with pathologic correlation. Radiology 187:493–501
4. Morrow M, Waters J, Morris E (2011) MRI for breast cancer screening, diagnosis, and treatment. Lancet 378:1804–1811
5. Morris EA (2007) Diagnostic breast MR imaging: current status and future directions. Radiol Clin North Am 45:863–880
6. Sardanelli F, Boetes C, Borisch B et al (2010) Magnetic resonance imaging of the breast: recommendations from the EUSOMA working group. Eur J Cancer 46:1296–1316
7. Yerushalmi R, Kennecke H, Woods R, Olivotto IA, Speers C, Gelmon KA (2009) Does multicentric/multifocal breast cancer

differ from unifocal breast cancer? An analysis of survival and contralateral breast cancer incidence. Breast Cancer Res Treat 117:365–370
8. Houssami N, Ciatto S, Macaskill P et al (2008) Accuracy and surgical impact of magnetic resonance imaging in breast cancer staging: systematic review and meta-analysis in detection of multifocal and multicentric cancer. J Clin Oncol 26:3248–3258
9. American Joint Committee on Cancer, (2010) Breast. In: Edge SB, Byrd DR, Compton CC (eds) AJCC cancer staging manual. Springer, New York, pp 347–376
10. Weissenbacher TM, Zschage M, Janni W et al (2010) Multicentric and multifocal versus unifocal breast cancer: is the tumor-node-metastasis classification justified? Breast Cancer Res Treat 122: 27–34
11. Pinker K, Bickel H, Helbich TH et al (2013) Combined contrast-enhanced magnetic resonance and diffusion-weighted imaging reading adapted to the "Breast Imaging Reporting and Data System" for multiparametric 3-T imaging of breast lesions. Eur Radiol 23:1791–1802
12. Pinker K, Bogner W, Baltzer P et al (2014) Improved diagnostic accuracy with multiparametric magnetic resonance imaging of the breast using dynamic contrast-enhanced magnetic resonance imaging, diffusion-weighted imaging, and 3-dimensional proton magnetic resonance spectroscopic imaging. Invest Radiol 49:421–430
13. Partridge SC, DeMartini WB, Kurland BF, Eby PR, White SW, Lehman CD (2009) Quantitative diffusion-weighted imaging as an adjunct to conventional breast MRI for improved positive predictive value. AJR Am J Roentgenol 193:1716–1722
14. Ei Khouli RH, Jacobs MA, Mezban SD et al (2010) Diffusion-weighted imaging improves the diagnostic accuracy of conventional 3.0-T breast MR imaging. Radiology 256:64–73
15. Spick C, Pinker-Domenig K, Rudas M, Helbich TH, Baltzer PA (2014) MRI-only lesions: application of diffusion-weighted imaging obviates unnecessary MR-guided breast biopsies. Eur Radiol 24:1204–1210
16. Morris EA, Comstock CE, Lee CH et al (2013) ACR BI-RADS magnetic resonance imaging. In: ACR BI-RADS® Atlas, Breast Imaging Reporting and Data System. Reston, VA: American College of Radiology.
17. Eby PR, DeMartini WB, Gutierrez RL, Saini MH, Peacock S, Lehman CD (2009) Characteristics of probably benign breast MRI lesions. Am J Roentgenol 193:861–867
18. Mahoney MC, Gatsonis C, Hanna L, DeMartini WB, Lehman C (2012) Positive predictive value of BI-RADS MR imaging. Radiology 264:51–58
19. Egan RL (1982) Multicentric breast carcinomas: clinical-radiographic-pathologic whole organ studies and 10-year survival. Cancer 49:1123–1130
20. Lim HI, Choi JH, Yang JH et al (2010) Does pre-operative breast magnetic resonance imaging in addition to mammography and breast ultrasonography change the operative management of breast carcinoma? Breast Cancer Res Treat 119:163–167
21. Kul S, Cansu A, Alhan E, Dinc H, Gunes G, Reis A (2011) Contribution of diffusion-weighted imaging to dynamic contrast-enhanced MRI in the characterization of breast tumors. AJR Am J Roentgenol 196:210–217
22. Chen X, Li WL, Zhang YL, Wu Q, Guo YM, Bai ZL (2010) Meta-analysis of quantitative diffusion-weighted MR imaging in the differential diagnosis of breast lesions. BMC Cancer 10:693
23. Tsushima Y, Takahashi-Taketomi A, Endo K (2009) Magnetic resonance (MR) differential diagnosis of breast tumors using apparent diffusion coefficient (ADC) on 1.5-T. J Magn Reson Imaging: JMRI 30:249–255
24. Cakir O, Arslan A, Inan N et al (2013) Comparison of the diagnostic performances of diffusion parameters in diffusion weighted imaging and diffusion tensor imaging of breast lesions. Eur J Radiol 82:e801–e806
25. Nijenhuis MV, Rutgers EJ (2015) Conservative surgery for multifocal/multicentric breast cancer. Breast 24:S96–S99